



RESEARCH PAPER

Genomic comparison of two independent seagrass lineages reveals habitat-driven convergent evolution

HueyTyng Lee^{1,2}, Agnieszka A. Golicz³, Philipp E. Bayer², Anita A. Severn-Ellis²,
Chon-Kit Kenneth Chan², Jacqueline Batley², Gary A. Kendrick² and
David Edwards^{2,*}

¹ School of Agriculture and Food Sciences, University of Queensland, Brisbane, QLD 4072, Australia

² School of Biological Sciences, University of Western Australia, WA 6009, Australia

³ Plant Molecular Biology and Biotechnology Laboratory, Faculty of Veterinary and Agricultural Sciences, University of Melbourne, Parkville, Melbourne, VIC 3010, Australia

* Correspondence: dave.edwards@uwa.edu.au

Received 14 August 2017; Editorial decision 12 April 2018; Accepted 12 April 2018

Editor: Christine Raines, University of Essex, UK

Abstract

Seagrasses are marine angiosperms that live fully submerged in the sea. They evolved from land plant ancestors, with multiple species representing at least three independent return-to-the-sea events. This raises the question of whether these marine angiosperms followed the same adaptation pathway to allow them to live and reproduce under the hostile marine conditions. To compare the basis of marine adaptation between seagrass lineages, we generated genomic data for *Halophila ovalis* and compared this with recently published genomes for two members of Zosteraceae, as well as genomes of five non-marine plant species (*Arabidopsis*, *Oryza sativa*, *Phoenix dactylifera*, *Musa acuminata*, and *Spirodela polyrhiza*). *Halophila* and Zosteraceae represent two independent seagrass lineages separated by around 30 million years. Genes that were lost or conserved in both lineages were identified. All three species lost genes associated with ethylene and terpenoid biosynthesis, and retained genes related to salinity adaptation, such as those for osmoregulation. In contrast, the loss of the NADH dehydrogenase-like complex is unique to *H. ovalis*. Through comparison of two independent return-to-the-sea events, this study further describes marine adaptation characteristics common to seagrass families, identifies species-specific gene loss, and provides molecular evidence for convergent evolution in seagrass lineages.

Keywords: Gene loss, *Halophila ovalis*, marine adaptation, NDH complex, osmoregulation, seagrass, *Zostera muelleri*.

Introduction

Seagrasses are a polyphyletic group of flowering plants that live fully submerged in the marine environment and form monospecific meadows resembling terrestrial grasses. The morphology of seagrasses varies among species, though common features include long, strap-shaped leaves and simple flowers. Seagrasses belong to a basal lineage that diverged around 140

million years ago (Mya), before the divergence of the Poaceae within the monocotyledon clade. Although similar in form, seagrass species represent at least three independent return-to-the-sea events (Les *et al.*, 1997).

The convergent evolution of seagrasses is characterized by common physiological and morphological features that

Abbreviations: Mya, million years ago; NDH, NADH dehydrogenase-like; OGC, orthologous gene cluster; OGCsM, orthologous gene cluster with at least one gene originating from a monocot species; OGCZ, orthologous gene cluster unique to Zosteraceae; TAIR, The Arabidopsis Information Resource.

© The Author(s) 2018. Published by Oxford University Press on behalf of the Society for Experimental Biology.

This is an Open Access article distributed under the terms of the Creative Commons Attribution License (<http://creativecommons.org/licenses/by/4.0/>), which permits unrestricted reuse, distribution, and reproduction in any medium, provided the original work is properly cited.

possibly represent a collection of marine adaptation traits. For example, seagrass leaves lack stomata, and gas exchange occurs through permeable cuticles, while seagrass roots and rhizomes have aerenchyma to enhance gas transport. Seagrasses have also adapted to variable quality and low levels of light, which attenuates quickly in seawater (Larkum *et al.*, 2006; Strydom *et al.*, 2017) and have effective osmoregulation to survive in the saline aqueous environment (Koch *et al.*, 2007; Touchette, 2007). Seagrasses are adapted to aquatic reproduction, where the transport and capture of pollen grains is carried out on or below the water surface.

Current seagrass taxonomy contains around 72 species forming three families, Zosteraceae, Hydrocharitaceae and Cymodoceaceae complex (Les *et al.*, 1997; Short *et al.*, 2011; Nguyen *et al.*, 2015). Recent genome-wide comparative studies of two species in the Zosteraceae provided the first insight into genomic adaptation to the marine environment (Golicz *et al.*, 2015; Lee *et al.*, 2016; Olsen *et al.*, 2016). Genes associated with the synthesis and signalling of volatile substances, including ethylene, methyljasmonate, and terpenoids, were lost in both *Zostera muelleri* and *Z. marina*. Genes associated with morphological adaptation, including those for stomatal cell differentiation, flower development and pollen formation, were also absent or greatly reduced in number. An increase in gene families associated with low light harvesting and cell wall modification was observed and postulated to contribute to survival in the light-attenuated and high salinity environment.

These gene losses, gene modifications, and gene family expansions in the two *Zostera* species may not reflect the independent adaptation of other seagrass lineages to the marine environment, and analysis of a second lineage is required to answer the question whether they share a common adaptation pathway to the ocean. *Halophila ovalis* is a seagrass species in the family Hydrocharitaceae, and is an ideal model for comparison with the *Zostera* species. The seagrass subclade in Hydrocharitaceae is embedded within branches of largely diverse aquatic angiosperms, including freshwater species (Larkum *et al.*, 2006), indicating the independent rise of marine adaption phenotypes.

As the likelihood of convergent evolution is predicted to decrease with phylogenetic distance (Ord and Summers, 2015), the divergence time difference between the seagrass subclade in Hydrocharitaceae (55 Mya; Chen *et al.*, 2012) and Zosteraceae (25 Mya; Coyer *et al.*, 2013) highlights the importance of this study. Moreover, since examples of parallel evolution, where similar phenotypes are generated from a similar genetic process of independent convergent evolution (Ord and Summers, 2015), are not abundant in plants (examples include carnivorous species (Fukushima *et al.*, 2017), recurrence of C4 photosynthesis (reviewed in Washburn *et al.*, 2016) and convergent mutations in loci during domestication (Paterson *et al.*, 1995)), and that habitat is the most common factor associated with reported examples of repeated evolution (Ord and Summers, 2015), independent seagrass lineages are excellent subjects for study.

In this work, a genomic comparison between seagrasses of Hydrocharitaceae and Zosteraceae was explored to determine whether the gene loss previously identified in *Z. muelleri* and

Z. marina is also observed in *H. ovalis*. We also attempt to identify any seagrass-specific genes that are present in one or both lineages. *Halophila ovalis* genome sequencing data were compared with the annotated genomes of *Z. marina* and *Z. muelleri*, together with representative land plants. Our study demonstrates that lost genes associated with the synthesis and signalling of volatile substances, as well as stomatal development, are shared by both seagrass lineages. Genes that are uniquely conserved across the two lineages are enriched in pathways related to cell osmoregulation, and provide molecular evidence for independent marine colonization. Results also revealed the loss of the NADH dehydrogenase-like (NDH) protein complex in *H. ovalis*, a characteristic that is not shared by the other two seagrass species. This study provides a more complete description of marine adaptation, and suggest a parallel convergent evolution of two independent return-to-the-sea events in seagrasses separated by 30 million years.

Materials and methods

Genome sequencing of *H. ovalis*

One *H. ovalis* plant sample was collected at Swan River, Claremont, Perth, Western Australia (coordinates: 32° 0' 3.98" S, 115° 45' 18.31" E).

The growth tips of the seagrass thalli were carefully removed, rinsed in sterile water, and inspected for visible external contamination. Seven hundred milligrams of tissue was placed in 5 ml tubes, flash frozen in liquid nitrogen, and bead-pulverized using a 2010 Geno/Grinder (SPEX SamplePrep, USA). The Qiagen DNeasy Plant Mini Kit was used for the extraction of the DNA. The frozen powdered plant material was suspended in 3 ml of Buffer AP1 and 28 µl of RNase A was added. After incubating at 65 °C, 910 µl of Buffer AP2 was added. The tubes were incubated on ice for 5 min and centrifuged thereafter to collect plant debris. Lysate (450 µl) was transferred to each of five to six QIAshredder tubes. The remainder of the DNA extraction steps were followed according to the kit protocol. The extracted DNA of each repetition was pooled after elution. DNA concentration was quantified using a Qubit 3.0 Fluorometer (Thermo Fisher Scientific) and visualized using a Labchip GX Touch 24 (PerkinElmer).

The extracted DNA was submitted to the Australian Genome Research Facility (AGRF) for library preparation and whole genome sequencing. The libraries for genome sequencing were prepared using the Illumina TruSeq Nano DNA HT Library Preparation Kit, according to the manufacturer's instructions. Genomic DNA was sequenced using an Illumina HiSeqX sequencer with 150 bp paired-end technology at the Garvan Institute of Medical Research.

A total of 510 485 779 paired-end reads were sequenced. Based on previous flow cytometry analysis of two other Hydrocharitaceae members, *Najas minor* (2C=7.28) and *Eldodea Canadensis* (2C=7.54) (Hidalgo *et al.*, 2015), as well as genome size prediction (3 628 962 593 bp, $k=45$) using the software Kmergenie (Chikhi and Medvedev, 2014) the sequencing coverage was estimated as ~40×. The sequences were deposited in a public repository (NCBI BioProject Accession PRJNA396090). Clones and low quality reads were removed using Sickle (Joshi and Fass, 2011).

Pipeline to identify lost and conserved genes

The identification of lost and conserved genes was achieved using the mapping of whole genome shotgun sequencing reads against reference genomes based on a previous approach (Golicz *et al.*, 2015). The reads were mapped to coding sequences (CDS) of reference species using dc-megaBLAST (Camacho *et al.*, 2009) with e-value 1e-5. A custom python script, calculate_blast_coverage.py (downloadable at https://github.com/AppliedBioinformatics/H_ovalis_supplementary.git), was used to calculate the horizontal coverage of each CDS. The average coverage of each

CDS across multiple reference species was calculated. If the average coverage was <2%, which means that mapped reads covered less than 2% of the length of a CDS, the orthologue was considered lost. If the average coverage was >50%, the orthologue was conserved.

Orthologous gene cluster construction

A set of 16 007 orthologous gene clusters (OGCs) conserved between seven model species with at least one gene originating from a monocot species, termed OGCsM (as defined in Table S1 in Golicz *et al.*, 2015), was used to represent orthologues highly conserved in plants.

Gene clusters unique to *Zosteraceae* were identified using all-against-all comparison with BLASTP (Camacho *et al.*, 2009) using the following parameters: 'blastp -evalue 1e-5', followed by OrthoMCL (Li *et al.*, 2003) between *Z. muelleri*, *Z. marina*, one dicot (*Arabidopsis*), and three other monocots (*Oryza sativa*, *Musa acuminata*, and *Spirodela polyrhiza*) (species selection based on Lee *et al.*, 2016). This group of orthologous genes was termed OGCZ.

Lost and conserved *H. ovalis*, *Z. muelleri* and *Z. marina* genes in OGCsM

Primary transcript CDSs of five species (four land plants: *Arabidopsis*, *Oryza sativa*, *Musa acuminata*, and *Phoenix dactylifera*; one floating freshwater plant: *Spirodela polyrhiza*; versions as listed in Golicz *et al.*, 2015) were used as references for mapping of reads from *H. ovalis*. Presence and absence results from a previous publication were used for *Z. muelleri* and *Z. marina* (Golicz *et al.*, 2015). For each orthologue in OGCsM, lost or conserved status was assigned in each species.

Lost and conserved *H. ovalis* genes in OGCZ

Primary transcript CDSs of *Z. muelleri* (http://www.appliedbioinformatics.com.au/index.php/Seagrass_Zmu_Genome; Lee *et al.*, 2016) and *Z. marina* (Phytozome 10; Olsen *et al.*, 2016) were used as references for *H. ovalis* read mapping. For each orthologue in OGCZ, lost or conserved status was assigned in *H. ovalis*.

Gene ontology enrichment and word cloud plotting

GO annotation and enrichment were performed using the topGO package (Alexa and Rahnenfuhrer, 2010) based on a previous approach (Golicz *et al.*, 2015). OGCsM was used as background, except for the GO enrichment of OGCZ genes where *Arabidopsis* whole proteome (TAIR10) was used.

A word cloud was generated and coloured to represent the enriched significance of GO terms using the wordcloud package (Fellows, 2014).

Inferring gene function through the level of protein domain conservation

OGCZ proteins of *Z. muelleri*, *Z. marina* and *Arabidopsis* were compared with TIGRFAM, ProDom, Panther, PfamA and PrositePatterns using InterProScan (version 5.14; Jones *et al.*, 2014) for motif and domain annotation. Domains of each protein were assigned with InterProScan IDs. The InterProScan IDs were compared between *Arabidopsis* and *Zosteraceae* genes for each OGCZ cluster.

Assembly of *H. ovalis* protein and multiple sequence alignments with orthologues of other species

Halophila ovalis reads aligned to CDS of 50S ribosomal protein L16 were extracted and assembled using Spades v3.10.1 (Bankevich *et al.*, 2012) with the following commands: spades.py, only-assembler, 1 reads_1.fasta, 2 reads_2.fasta. Corresponding protein was aligned to the assembled contigs using Exonerate (Slater and Birney, 2005) with the following parameters: exonerate, model protein2genome, E 1, bestn 1, score 100, softmaskquery no, softmasktarget yes, minintron 20, maxintron 20000,

ryo ">HAL_%qi_%qd\n%tas". The aligned target regions were translated to protein sequences using the translate tool in ExPASy (Gasteiger *et al.*, 2003). Each *H. ovalis* protein sequence obtained was aligned with orthologues of selected species (Table S1 at JXB online) using MAFFT (Katoh *et al.*, 2002). A phylogenetic tree was plotted with PhyML (Guindon *et al.*, 2009) assuming the JTT model for amino acid substitution and gamma parameter for invariable sites (based on Huang *et al.*, 2016) using the alignments excluding the outgroup (charophyte and chlorophyte). The multiple-sequence alignments were visualized and coloured using Jalview (Waterhouse *et al.*, 2009).

Results

Read alignment of *H. ovalis* to reference species CDS

A total of 112 202 319 *H. ovalis* reads (10.9%) were discarded in the process of clonal removal and quality-based filtering (Table S2). Out of the remaining 908 769 239 *H. ovalis* reads, 2.7% (24 495 631) aligned to *Arabidopsis* CDS, 5.6% (50 565 060) aligned to *Oryza sativa* CDS, 1.3% (11 617 255) aligned to *Musa acuminata* CDS, 0.8% (7 367 361) aligned to *Phoenix dactylifera* CDS and 1.8% (16 600 802) aligned to *Spirodela polyrhiza* CDS. For the seagrass reference species, 1.8% (16 727 940) and 0.5% (5 005 993) of *H. ovalis* reads aligned to *Z. muelleri* and *Z. marina* CDSs, respectively.

Conservation of core biological processes

A total of 4367 OGCsM genes, out of 16 007, were conserved in *H. ovalis*. When compared with conserved genes previously described in *Z. muelleri* and *Z. marina* (Golicz *et al.*, 2015; Lee *et al.*, 2016; Olsen *et al.*, 2016), 3335 (76.4%) genes were conserved in all three seagrass species, 377 genes were shared with either *Z. muelleri* or *Z. marina*, and 655 genes were only conserved in *H. ovalis*. A total of 508 genes were only conserved in the *Zosteraceae* species. A full list of genes conserved in *H. ovalis* and their presence in other seagrass species is presented in Table S3. The GO terms enriched in these 4367 OGCsM genes conserved in *H. ovalis* involved core biological pathways such as photosynthesis, chlorophyll biosynthesis, and glycolytic processes, as well as response to stresses such as cadmium (Table 1).

Gene loss in *H. ovalis* and comparison of lost genes between the three seagrass species

A total of 1822 OGCsM genes were lost in *H. ovalis*, and these were compared with those previously reported as lost in both *Z. muelleri* and *Z. marina* (Golicz *et al.*, 2015; Lee *et al.*, 2016; Olsen *et al.*, 2016) (Table S4). A total of 1197 (65.6%) lost genes were shared between all three seagrass species, 187 were shared with either *Z. muelleri* or *Z. marina*, and 412 were only lost in *H. ovalis*. In comparison, 743 genes were only lost in the *Zosteraceae* lineage. Enriched GO terms for the 1822 OGCsM genes highlighted the loss of genes associated with ethylene synthesis and perception, and stomatal development (Table 2). The presence or absence of genes involved in stomatal development, ethylene synthesis and signalling, and terpenoid biosynthesis in *H. ovalis*, *Z. marina*, and *Z. muelleri* are listed in Table 3.

Table 1. Significantly enriched biological process GO terms in the genes conserved in *H. ovalis* compared with five other plant species (*Arabidopsis*, *Oryza sativa*, *Musa acuminata*, *Phoenix dactylifera*, and *Spirodela polyrhiza*)

| GO ID | Term | P value |
|------------|---|-----------------------|
| GO:0046686 | Response to cadmium ion | 3.0×10^{-30} |
| GO:0006412 | Translation | 4.1×10^{-28} |
| GO:0046496 | Nicotinamide nucleotide metabolic process | 3.9×10^{-16} |
| GO:0006099 | Tricarboxylic acid cycle | 1.7×10^{-13} |
| GO:0015991 | ATP hydrolysis-coupled proton transport | 1.0×10^{-12} |
| GO:1901566 | Organonitrogen compound biosynthetic process | 7.9×10^{-11} |
| GO:0043039 | tRNA aminoacylation | 1.2×10^{-10} |
| GO:0006090 | Pyruvate metabolic process | 1.9×10^{-10} |
| GO:1901293 | Nucleoside phosphate biosynthetic process | 2.3×10^{-10} |
| GO:0009156 | Ribonucleoside monophosphate biosynthetic process | 2.7×10^{-10} |
| GO:0009225 | Nucleotide-sugar metabolic process | 5.4×10^{-10} |
| GO:0007264 | Small GTPase-mediated signal transduction | 8.2×10^{-9} |
| GO:0046034 | ATP metabolic process | 8.4×10^{-9} |
| GO:0006108 | Malate metabolic process | 1.4×10^{-8} |
| GO:0006006 | Glucose metabolic process | 1.8×10^{-8} |
| GO:0034622 | Cellular macromolecular complex assembly | 2.3×10^{-8} |
| GO:0071702 | Organic substance transport | 2.4×10^{-8} |
| GO:0018105 | Peptidyl-serine phosphorylation | 3.2×10^{-8} |
| GO:0009250 | Glucan biosynthetic process | 2.0×10^{-7} |
| GO:0016192 | Vesicle-mediated transport | 2.0×10^{-7} |
| GO:0010499 | Proteasomal ubiquitin-independent protein catabolic process | 3.4×10^{-7} |
| GO:0043094 | Cellular metabolic compound salvage | 6.7×10^{-7} |
| GO:0015994 | Chlorophyll metabolic process | 1.2×10^{-6} |
| GO:0034613 | Cellular protein localization | 1.4×10^{-6} |
| GO:0006536 | Glutamate metabolic process | 1.9×10^{-6} |
| GO:0005985 | Sucrose metabolic process | 5.3×10^{-6} |
| GO:0098656 | Anion transmembrane transport | 5.7×10^{-6} |
| GO:0015672 | Monovalent inorganic cation transport | 7.5×10^{-6} |
| GO:0009932 | Cell tip growth | 9.9×10^{-6} |
| GO:0006081 | Cellular aldehyde metabolic process | 1.0×10^{-5} |
| GO:0018298 | Protein–chromophore linkage | 1.0×10^{-5} |
| GO:0030163 | Protein catabolic process | 1.3×10^{-5} |
| GO:0048588 | Developmental cell growth | 1.3×10^{-5} |
| GO:0006102 | Isocitrate metabolic process | 2.4×10^{-5} |
| GO:0006607 | NLS-bearing protein import into nucleus | 2.5×10^{-5} |
| GO:0015977 | Carbon fixation | 5.1×10^{-5} |
| GO:0015979 | Photosynthesis | 5.4×10^{-5} |
| GO:0006563 | L-Serine metabolic process | 6.0×10^{-5} |
| GO:0006268 | DNA unwinding involved in DNA replication | 6.9×10^{-5} |
| GO:0007035 | Vacuolar acidification | 6.9×10^{-5} |
| GO:0009768 | Photosynthesis, light harvesting in photosystem I | 7.2×10^{-5} |
| GO:0016197 | Endosomal transport | 8.1×10^{-5} |
| GO:0030048 | Actin filament-based movement | 0.00012 |
| GO:0009651 | Response to salt stress | 0.00012 |
| GO:0006206 | Pyrimidine nucleobase metabolic process | 0.00013 |
| GO:0030243 | Cellulose metabolic process | 0.00014 |
| GO:0097164 | Ammonium ion metabolic process | 0.00015 |
| GO:0010315 | Auxin efflux | 0.00015 |
| GO:0006551 | Leucine metabolic process | 0.00017 |
| GO:0006085 | Acetyl-CoA biosynthetic process | 0.00018 |
| GO:0045899 | Positive regulation of RNA polymerase II transcriptional preinitiation complex assembly | 0.00020 |
| GO:0032012 | Regulation of ARF protein signal transduction | 0.00020 |
| GO:0009735 | Response to cytokinin | 0.00027 |

Table 1. Continued

| GO ID | Term | P value |
|------------|--|---------|
| GO:0006782 | Protoporphyrinogen IX biosynthetic process | 0.00030 |
| GO:0009846 | Pollen germination | 0.00032 |
| GO:1901679 | Nucleotide transmembrane transport | 0.00041 |
| GO:0030042 | Actin filament depolymerization | 0.00048 |
| GO:0006558 | L-Phenylalanine metabolic process | 0.00050 |
| GO:0006544 | Glycine metabolic process | 0.00057 |
| GO:0035999 | Tetrahydrofolate interconversion | 0.00096 |
| GO:0009066 | Aspartate family amino acid metabolic process | 0.00103 |
| GO:0006222 | UMP biosynthetic process | 0.00113 |
| GO:0046500 | S-Adenosylmethionine metabolic process | 0.00125 |
| GO:0015804 | Neutral amino acid transport | 0.00125 |
| GO:0006097 | Glyoxylate cycle | 0.00125 |
| GO:0030433 | Endoplasmic reticulum-associated ubiquitin-dependent protein degradation | 0.00132 |
| GO:0019627 | Urea metabolic process | 0.00169 |
| GO:0015800 | Acidic amino acid transport | 0.00169 |
| GO:0000398 | mRNA splicing, via spliceosome | 0.00170 |
| GO:0010540 | Basipetal auxin transport | 0.00235 |
| GO:0035435 | Phosphate ion transmembrane transport | 0.00258 |
| GO:0006457 | Protein folding | 0.00262 |
| GO:0051259 | Protein oligomerization | 0.00265 |
| GO:0006525 | Arginine metabolic process | 0.00265 |
| GO:0016482 | Cytoplasmic transport | 0.00284 |
| GO:0016036 | Cellular response to phosphate starvation | 0.00288 |
| GO:0043604 | Amide biosynthetic process | 0.00295 |
| GO:0019395 | Fatty acid oxidation | 0.00317 |
| GO:0006570 | Tyrosine metabolic process | 0.00326 |
| GO:0052646 | Alditol phosphate metabolic process | 0.00326 |
| GO:0010043 | Response to zinc ion | 0.00346 |
| GO:0055085 | Transmembrane transport | 0.00377 |
| GO:0000338 | Protein deneddylation | 0.00436 |
| GO:0006002 | Fructose 6-phosphate metabolic process | 0.00436 |
| GO:0043650 | Dicarboxylic acid biosynthetic process | 0.00439 |
| GO:0010501 | RNA secondary structure unwinding | 0.00439 |
| GO:0009629 | Response to gravity | 0.00447 |
| GO:0006103 | 2-Oxoglutarate metabolic process | 0.00490 |
| GO:0009833 | Plant-type primary cell wall biogenesis | 0.00490 |
| GO:0006610 | Ribosomal protein import into nucleus | 0.00490 |
| GO:0010541 | Acropetal auxin transport | 0.00540 |
| GO:0006012 | Galactose metabolic process | 0.00540 |
| GO:0006511 | Ubiquitin-dependent protein catabolic process | 0.00630 |
| GO:0051275 | β-Glucan catabolic process | 0.00735 |
| GO:0009141 | Nucleoside triphosphate metabolic process | 0.00770 |
| GO:0018208 | Peptidyl-proline modification | 0.00803 |
| GO:0006486 | Protein glycosylation | 0.00804 |
| GO:0009624 | Response to nematode | 0.00847 |
| GO:1904659 | Glucose transmembrane transport | 0.00872 |
| GO:0046323 | Glucose import | 0.00872 |
| GO:0006631 | Fatty acid metabolic process | 0.00878 |
| GO:0044282 | Small molecule catabolic process | 0.00886 |

Halophila ovalis lost genes encoding NADH dehydrogenase-like complex assembly

The five most significantly enriched GO terms in the 412 genes that were only lost in *H. ovalis* were cellular response to light intensity (GO:0071484), cellular response to UV (GO:0034644), photosynthetic electron transport in

Table 2. Significantly enriched biological process GO terms in the genes conserved in five other plant species (*Arabidopsis*, *Oryza sativa*, *Musa acuminata*, *Phoenix dactylifera* and *Spirodela polyrhiza*) but absent in *H. ovalis*

| Function | GO ID | Term | P value |
|-----------------------------------|------------|--|-----------------------|
| Ethylene synthesis and signalling | GO:0009835 | Fruit ripening | 4.1×10^{-10} |
| | GO:0042218 | 1-Aminocyclopropane-1-carboxylate biosynthetic process | 6.3×10^{-10} |
| | GO:0009693 | Ethylene biosynthetic process | 1.9×10^{-8} |
| | GO:0010105 | Negative regulation of ethylene-activated signalling pathway | 1.2×10^{-6} |
| Stomata development | GO:0010375 | Stomatal complex patterning | 0.00012 |
| | GO:2000038 | Regulation of stomatal complex development | 0.00608 |
| Others | GO:0045168 | Cell–cell signalling involved in cell fate commitment | 3.1×10^{-6} |
| | GO:0006952 | Defence response | 9.4×10^{-6} |
| | GO:0009626 | Plant-type hypersensitive response | 1.0×10^{-5} |
| | GO:0031640 | Killing of cells of other organism | 8.4×10^{-5} |
| | GO:0010039 | Response to iron ion | 0.00011 |
| | GO:0034644 | Cellular response to UV | 0.00014 |
| | GO:0071484 | Cellular response to light intensity | 0.00018 |
| | GO:0009773 | Photosynthetic electron transport in photosystem I | 0.00023 |
| | GO:0080027 | Response to herbivore | 0.00034 |
| | GO:0033473 | Indoleacetic acid conjugate metabolic process | 0.00034 |
| | GO:0009696 | Salicylic acid metabolic process | 0.00059 |
| | GO:0033609 | Oxalate metabolic process | 0.00093 |
| | GO:0050832 | Defence response to fungus | 0.00113 |
| | GO:0071423 | Malate transmembrane transport | 0.00209 |
| | GO:0042542 | Response to hydrogen peroxide | 0.00234 |
| | GO:1900426 | Positive regulation of defence response to bacterium | 0.00239 |
| | GO:0010876 | Lipid localization | 0.00313 |
| | GO:0018106 | Peptidyl-histidine phosphorylation | 0.00404 |
| | GO:0046688 | Response to copper ion | 0.00558 |
| | GO:0010257 | NADH dehydrogenase complex assembly | 0.00608 |
| | GO:0009838 | Abscission | 0.00704 |
| | GO:0071732 | Cellular response to nitric oxide | 0.00791 |

photosystem I (GO:0009773), NADH dehydrogenase complex assembly (GO:0010257), and cellular response to salt stress (GO:0071472). A complete list of all significantly enriched terms is given in Table S5. Closer examination revealed the loss of 23 (15 nuclear and 8 chloroplast) genes that encode the five subcomplexes in the NDH complex (Table 4). In addition, 17 genes required for the supercomplex formation, including tethering of NDH to photosystem I, assembly of subunits, accessory proteins, and transcription factors, were absent in *H. ovalis*. Two proteins required for nitrate uptake and assimilation, nitrogen reductase 1 (NR1) and nitrate transporter (NRT3.1), were also lost in *H. ovalis*.

Co-evolution of genes for intracellular transport, cell wall, and ion transport-related genes in *H. ovalis* and *Zostera*

We identified a set of 1748 genes that are unique to *Z. muelleri* and *Z. marina*, termed OGCZ (Fig. S1; Table S6), with 57 also found to be conserved in *H. ovalis* (Table S7). Putative functions of these 57 genes were inferred by matching their protein domains to the corresponding best aligned *Arabidopsis* gene. Out of 57 OGCZ groups, 45 have identical domains (indicated as InterProScan IDs) to the corresponding *Arabidopsis* genes. A total of eight of them have fewer or different domains from *Arabidopsis*, and four of them have no domains assigned (Table S7).

The majority of the 57 OGCZ genes conserved in *H. ovalis* are predicted to be involved in protein secretion and

intracellular transport, with significantly enriched terms annotated with cellular component ontology, including organelles of the intracellular transport pathways, namely Golgi apparatus, trans-Golgi network, and endosome, and nearly half of the remaining terms intracellular transport-related (Fig. 1). A total of 13 genes are predicted to function in protein secretion and intracellular transport, mainly as transport proteins or transport regulators. Nine genes are associated with cell wall construction, organization, and modification, while other predicted functions include ion or proton transport, lipid catabolism, transcription and translation-related, protein ubiquitination, and histone assembly (Table 5).

Molecular comparison of seagrass ribosomal proteins

Ribosomal 50S L16 orthologues from the two *Zostera* species, *H. ovalis*, and 12 species in the Alismatales order were aligned, together with predicted proteins from five model land plants (Table S1). We identified nine amino acid positions that appear to be specific to the seagrasses *H. ovalis*, *Z. muelleri*, and *Z. marina* (white arrows in Fig. 2) and conserved among the other 17 angiosperms (12 belong to the Alismatales order, eight are freshwater plants), one charophyte and one chlorophyte.

A phylogenetic tree for these 22 species based on this protein sequence, which describes the relationships between orthologues of these 22 species, separates the seagrass species (*H. ovalis*, *Z. muelleri*, and *Z. marina*) from the other species (Fig. 3). The separation of the two *Zostera* orthologues from

Table 3. Presence and absence of genes involved in stomatal development, ethylene synthesis and signalling, and terpenoid biosynthesis in OGCsM, *H. ovalis*, *Z. marina*, and *Z. muelleri*

| Gene ID | Protein name | Function | Conserved in OGCsM | Presence in <i>H. ovalis</i> | Presence in <i>Z. muelleri</i> | Presence in <i>Z. marina</i> |
|-----------------------------------|--------------|------------------------|--------------------|------------------------------|--------------------------------|------------------------------|
| Stomata development | | | | | | |
| AT1G04110 | SBT1.2 | Spacing and patterning | + | NA | – | – |
| AT4G12970 | EPFL9 | Spacing and patterning | + | – | – | – |
| AT2G20875 | EPF1 | Spacing and patterning | + | – | – | – |
| AT1G80080 | TMM | Spacing and patterning | + | – | – | – |
| AT1G34245 | EPF2 | Spacing and patterning | + | – | – | – |
| AT2G02820 | MYB88 | Differentiation | – | NA | NA | – |
| AT3G06120 | MUTE | Differentiation | + | – | – | – |
| AT5G53210 | SPCH | Differentiation | + | – | – | – |
| AT3G24140 | FAMA | Differentiation | + | NA | NA | – |
| AT1G12860 | SCRM2 | Differentiation | – | NA | NA | – |
| AT1G14350 | FLP | Differentiation | + | – | – | – |
| Ethylene synthesis and signalling | | | | | | |
| AT2G19590 | ACO1 | ACC oxidase | + | – | – | – |
| AT1G62380 | ACO2 | ACC oxidase | + | – | – | – |
| AT1G05010 | ACO4 | ACC oxidase | + | – | – | – |
| AT1G77330 | ACO5 | ACC oxidase | + | – | – | – |
| AT3G61510 | ACS1 | ACC synthase | + | – | – | – |
| AT1G01480 | ACS2 | ACC synthase | + | – | – | – |
| AT2G22810 | ACS4 | ACC synthase | + | – | – | – |
| AT5G65800 | ACS5 | ACC synthase | + | – | – | – |
| AT4G11280 | ACS6 | ACC synthase | + | – | – | – |
| AT4G26200 | ACS7 | ACC synthase | + | – | – | – |
| AT4G37770 | ACS8 | ACC synthase | + | – | – | – |
| AT3G49700 | ACS9 | ACC synthase | + | – | – | – |
| AT4G08040 | ACS11 | ACC synthase | + | – | – | – |
| AT2G40940 | ERS1 | Ethylene receptor | + | – | – | – |
| AT1G66340 | ETR1 | Ethylene receptor | + | – | – | – |
| AT3G23150 | ETR2 | Ethylene receptor | + | – | – | – |
| AT3G04580 | EIN4 | Ethylene receptor | + | – | – | – |
| AT5G03730 | CTR1 | Raf-like kinase | + | NA | NA | – |
| AT5G03280 | EIN2 | Signal transducer | + | NA | – | – |
| AT2G25490 | EBF1 | EIN2 degradation | + | – | – | – |
| AT5G25350 | EBF2 | EIN2 degradation | + | – | – | – |
| Terpenoid biosynthesis | | | | | | |
| AT3G25820 | TPS-CIN | Terpene synthase | + | – | – | – |
| AT3G25830 | TPS23 | Terpene synthase | + | – | – | – |
| AT4G16740 | TPS03 | Terpene synthase | – | – | – | – |
| AT2G24210 | TPS10 | Terpene synthase | + | – | – | – |
| AT3G25810 | TPS24 | Terpene synthase | – | – | – | – |

Categories are: gene present (+), gene absent (–), and information not available (NA).

H. ovalis is also well-supported. Sister genera of both *Halophila* and *Zostera* grouped together as members of core alismatids (red in Fig. 3) (Alismatidae *sensu*; Les and Tippery, 2013).

Discussion

The concurrent absence of multiple genes in *H. ovalis*, *Z. muelleri*, and *Z. marina* suggests independently evolved convergent adaptation of seagrasses to the marine environment. Seagrass leaves lack stomata and the flowers have simplified structures when compared with terrestrial angiosperms (Kuo and Hartog, 2006). The loss of genes in stomata patterning and differentiation, and in sepal and petal development was previously described in *Zostera*, together with the loss of gaseous

hormones and metabolites, such as ethylene, methyl jasmonate, and secondary volatile terpenes (Golicz et al., 2015; Lee et al., 2016; Olsen et al., 2016). Consistent with the low diffusion rate of gases underwater, the absence of ethylene production in seagrasses avoids accumulation in the tissues. In flood-adapted land plants, the ethylene signal is used to sense submergence and induces a response to flooding (Voesenek et al., 2015). Ethylene biosynthesis and signalling also play an important role in plant response to salinity (Zhang et al., 2016). There is conflicting evidence of ethylene as a positive or negative regulator during salinity stress in different species at different developmental stages (Tao et al., 2015), suggesting that some species adjust their sensitivity to environmental factors through regulation of the ethylene signalling pathway. As the loss of

Table 4. Presence and absence of 40 nuclear and chloroplast-encoded genes involved in formation of the NDH complex

| Gene ID | Protein name | Function | Presence in OGCsM | Presence in <i>H. ovalis</i> | Presence in <i>Z. muelleri</i> | Presence in <i>Z. marina</i> |
|---------------------|--------------|----------------------------|-------------------|------------------------------|--------------------------------|------------------------------|
| Nuclear encoded | | | | | | |
| AT1G70760 | NDHL | Subunit A | + | NA | + | + |
| AT4G37925 | NDHM | Subunit A | + | – | + | + |
| AT5G58260 | NDHN | Subunit A | + | NA | + | + |
| AT1G74880 | NDHO | Subunit A | + | – | + | + |
| AT4G23890 | NDHS | Subunit ED | + | – | NA | + |
| AT4G09350 | NDHT | Subunit ED | + | – | + | + |
| AT5G21430 | NDHU | Subunit ED | + | – | + | + |
| AT1G15980 | PNSB1 | Subunit B | + | – | NA | + |
| AT1G64770 | PNSB2 | Subunit B | + | – | + | + |
| AT3G16250 | PNSB3 | Subunit B | + | – | + | + |
| AT1G18730 | PNSB4 | Subunit B | + | – | + | + |
| AT2G39470 | PNSL1 | Subunit B | + | – | + | + |
| AT1G14150 | PNSL2 | Subunit L | + | – | + | + |
| AT3G01440 | PNSL3 | Subunit L | + | NA | + | + |
| AT4G39710 | PNSL4 | Subunit L | + | – | + | + |
| AT5G13120 | PNSL5 | Subunit L | + | + | + | + |
| AT2G47910 | CRR6 | Complex formation | + | – | + | + |
| AT5G39210 | CRR7 | Complex formation | + | – | + | + |
| AT1G45474 | Lhca5 | Complex formation | + | – | + | + |
| AT1G19150 | Lhca6 | Complex formation | + | NA | + | + |
| AT1G26230 | CRR27 | Complex formation | + | NA | + | + |
| AT1G51100 | CRR41 | Complex formation | + | NA | + | + |
| AT2G05620 | PGR5 | Proton gradient regulation | + | NA | + | + |
| AT4G22890 | PGRL1A | Proton gradient regulation | + | + | + | + |
| AT3G46790 | CRR2 | Unknown | + | NA | + | + |
| AT2G01590 | CRR3 | Unknown | + | – | – | + |
| AT5G20935 | CRR42 | Unknown | + | – | + | + |
| AT2G01918 | PQL3 | Unknown | + | – | – | + |
| AT1G55370 | NDF5 | Unknown | + | – | + | + |
| Chloroplast encoded | | | | | | |
| ATCG00890 | NDHB | Subunit M | + | NA | + | + |
| ATCG01250 | | | | | | |
| ATCG01010 | NDHF | Subunit M | + | NA | + | + |
| ATCG00440 | NDHC | Subunit M | + | – | + | + |
| ATCG01050 | NDHD | Subunit M | + | – | + | + |
| ATCG01070 | NDHE | Subunit M | + | – | + | + |
| ATCG01100 | NDHA | Subunit M | + | – | + | + |
| ATCG01080 | NDHG | Subunit M | + | NA | + | + |
| ATCG01110 | NDHH | Subunit A | + | + | + | + |
| ATCG00420 | NDHJ | Subunit A | + | – | + | + |
| ATCG00430 | NDHK | Subunit A | + | – | + | + |
| ATCG01090 | NDHI | Subunit A | + | – | + | + |

Categories are: gene present (+), gene absent (–), and information not available (NA).

ethylene genes is observed in both *H. ovalis* and *Zostera*, it is likely that ethylene is selected against during seagrass adaptation to a submerged marine lifestyle.

The sharing of OGCZ genes in *H. ovalis* to form a seagrass-specific gene set identifies orthologous relationships that appear to be unique to seagrass adaptation, despite their evolutionary distance and multiple origins. It is important to note that these 57 OGCZ genes are not novel genes but genes that have diverged sufficiently to cluster separately from other plants in orthologue analysis. The functions of these genes were not annotated but inferred by homology using annotated Arabidopsis genes. The majority of these genes are predicted to be involved in intracellular transport and in cell wall organization and modification.

In plant cells, secreted proteins are processed through the Golgi apparatus as cargo molecules and sorted by receptors in the trans-Golgi network to different destinations (Brandizzi and Barlowe, 2013). Non-cellulosic cell wall matrix polysaccharides are among the wide range of vesicles synthesized and transported by the Golgi apparatus (Driouich *et al.*, 1993; Lerouxel *et al.*, 2006; Driouich *et al.*, 2012). Besides catalytic mechanisms of glycosyltransferases and nucleotide-sugar conversions for polysaccharide assembly, the Golgi is also responsible for methylation of the cell wall polysaccharides. There are significant differences between cell walls of seagrasses and land plants. Seagrass cell walls contain sulfated polysaccharides (Aquino *et al.*, 2005) and seagrass pectin contains a rare class of apiose-substituted

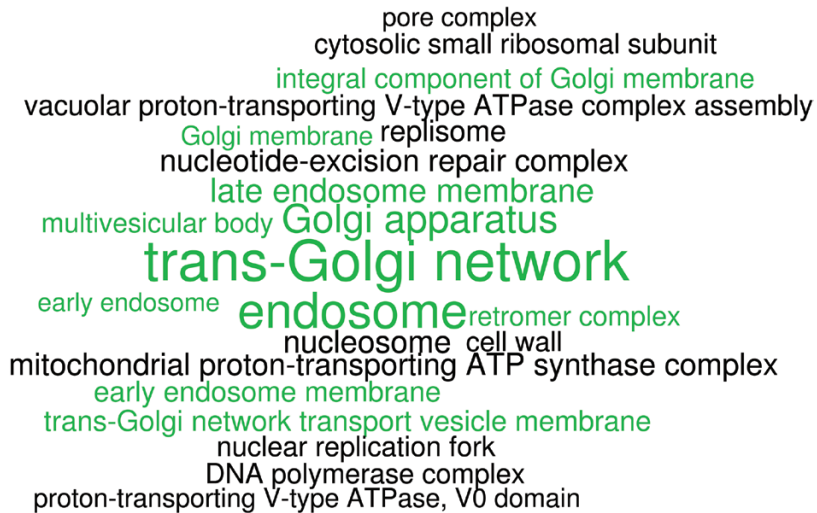


Fig. 1. Significantly enriched cellular component GO terms in seagrass-specific genes. Terms in green are subcomponents or organelles of the intracellular transport pathways.

homogalacturonan (Ovodov *et al.*, 1971) with low levels of methyl esterification (Khotimchenko *et al.*, 2012). These two modifications are thought to provide salt tolerance by increasing the polyanionic potential of cell walls (Aquino *et al.*, 2005, 2011; Olsen *et al.*, 2016). An expansion of pectin catabolic and methyltransferase genes was observed in the genomes of *Z. muelleri* (Lee *et al.*, 2016) and *Z. marina* (Olsen *et al.*, 2016), suggesting complex pectin modification in seagrasses. Interestingly, within the list of seagrass-specific genes conserved in *H. ovalis*, CGR2 (cotton Golgi-related 2), a methyltransferase, was shown to be involved in pectin methyltransferification in Arabidopsis (Weraduwege *et al.*, 2016). Tubulin cofactor, which is responsible for the stability of microtubules (Zhu *et al.*, 2015), is also found to be conserved among seagrasses. A total of five genes that encode RAB GTPases, the key regulators of vesicle trafficking (Miserey-Lenkei *et al.*, 2010; Valente *et al.*, 2010), were also conserved across both seagrass lineages. In Arabidopsis, knockouts of some members of the RAB GTPases have demonstrated roles in salinity stress tolerance (Asaoka *et al.*, 2013). It is likely that this conservation of cell wall-related genes, as well as proteins involved in intracellular transport, in both families of seagrasses is linked to modification of cell wall composition as one of the adaptations to osmotic stress.

Multiple salt-tolerance mechanisms have been hypothesized in seagrasses (reviewed in Touchette, 2007), including cell wall rigidity, selective ion flux and vacuolar ion sequestering, and the synthesis of compatible solutes and amino acids (Ye and Zhao, 2003; Carpaneto *et al.*, 2004; Touchette *et al.*, 2014; Cambridge *et al.*, 2017). To avoid salt damage, plant cells adjust osmotic balance through influx and efflux of ions through the transmembrane transport proteins, assisted by H⁺ pumps (Hasegawa, 2013). Three genes, namely a component of a vacuolar proton pump, ATP synthase and calmodulin, were identified as conserved across the two seagrass lineages. Moreover, vacuolar proton ATPase A1 has been shown to be responsive to salt stress in sugar beet (Kirsch *et al.*, 1996). This collection of genes may have a role in osmotic homeostasis of cells in the marine environment.

Lipid transport and catabolism is another important role of the intracellular transport system. The endoplasmic reticulum synthesizes and exports phospholipids, sterols, and storage lipids for various purposes, including formation of membrane structures (van Meer *et al.*, 2008). A total of four genes involved in lipid transport and catabolism were conserved in all three seagrass species, including ceramidase, which is responsible for sphingolipid metabolism. Sphingolipids provide membrane structure and are involved in cellular signal transduction (Hannun and Obeid, 2008). The difference between lipids of seagrasses and land plants is not well understood, but expansion in genes related to sphingolipid metabolism was observed in *Z. marina* when compared with duckweed (Olsen *et al.*, 2016). Another alkaline ceramidase had been shown to regulate cell turgor pressure in Arabidopsis (Chen *et al.*, 2015), but more evidence is needed to determine whether seagrass-specific lipid metabolism plays a role in marine adaptation.

Two members of the core histone family are conserved in seagrasses. The domains in histone families, particularly H2A and H3, demonstrate expansion in numbers and variety, but with strong conservation of each variant across species (Kawashima *et al.*, 2015). Ribosomal constituents were previously identified as modified in *Z. muelleri* when compared with land plants (Lee *et al.*, 2016) and positively selected in *Z. marina* and *P. oceanica* (Wissler *et al.*, 2011), and our results demonstrate that these genes are also conserved in *H. ovalis*. The basis for the observed differences in ribosomal gene sequences is not known, but it is postulated to be related to salt tolerance. Translation, and consequently protein synthesis are known to be salt-sensitive in yeast and plants (Rausell *et al.*, 2003). For example, the expression of genes encoding the translation apparatus was lower when the transcriptome of Arabidopsis was compared with the halophyte salt cress (Taji *et al.*, 2004). If seagrass ribosomes are adapted to relatively high salinity, this may have an application for improvement of salt tolerance in crop species.

Sequence variations were identified in chloroplast-encoded 50S ribosomal protein L16. Nine amino acid mutations were

Table 5. Fifty-seven orthologous groups of seagrass-specific genes shared in two *Zosteraceae* species (*Z. muelleri* and *Z. marina*) and *Halophila* categorized by predicted function

| Category of related function | Name of best TAIR10 hit corresponding to <i>Zostera</i> orthologue | ID of best TAIR10 hit corresponding to <i>Zostera</i> orthologue | Putative gene function |
|---|--|--|---|
| Protein secretion and intracellular transport | Endoplasmic reticulum retention defective 2B | AT3G25040.1 | Retention mechanism |
| | Endoplasmic reticulum-type calcium-transporting ATPase 3 | AT1G10130.1 | Calcium and manganese ion transport |
| | RAB GTPase homologue A1F | AT5G60860.1 | GTPase activity |
| | RAB GTPase homologue A2B | AT1G07410.1 | GTPase activity |
| | Secretory carrier 3 | AT1G61250.1 | Integral membrane protein |
| | NOD26-like intrinsic protein 1;2 | AT4G18910.1 | Aquaporin |
| | Mitochondrial substrate carrier family protein | AT3G53940.1 | Substrate transport |
| | Mitochondrial import inner membrane translocase subunit Tim17/Tim22/Tim23 family protein | AT5G63000.1 | Protein transport |
| | Transducin/WD40 repeat-like superfamily protein | AT3G01340.1 | Protein transport |
| | Protein of unknown function | AT1G09330.1 | — |
| Cell wall | Expansin A16 | AT3G55500.1 | Cell wall loosening |
| | Expansin A1 | AT1G69530.2 | Cell wall loosening |
| | Galacturonosyltransferase-like 2 | AT3G50760.1 | Cell wall organization |
| | Xyloglucan endotransglucosylase/hydrolase 5 | AT5G13870.1 | Cell wall organization |
| | Glucan synthase-like 8 | AT2G36850.1 | Callose synthesis |
| | S-Adenosyl-L-methionine-dependent methyltransferases superfamily protein | AT4G34050.1 | Lignin biosynthesis |
| | Peroxidase superfamily protein | AT5G05340.1 | Lignin biosynthesis |
| | Cotton Golgi-related 2 (pectin methyltransferase) | AT3G49720.1 | Cell wall modification |
| | Vascular related NAC-domain protein 1 | AT2G18060.1 | Xylem secondary cell wall formation |
| | ATP synthase epsilon chain, mitochondrial | AT1G51650.1 | Proton-transporting ATPase activity |
| Ion flux and sequestering | Vacuolar proton ATPase A1 | AT2G28520.1 | Proton-transporting ATPase activity |
| | Calmodulin 4 | AT1G66410.1 | Calcium ion binding |
| Lipid catabolism | Trigalactosyl-diacylglycerol 5 | AT1G27695.1 | Lipid transport |
| | GDSL-like lipase/acylhydrolase superfamily protein | AT1G29670.1 | Lipid catabolic process |
| | | AT5G45670.1 | |
| | Peroxin 6 | AT1G03000.1 | Peroxisomal matrix protein import |
| Transcription-related | Alkaline phytoceramidase | AT4G22330.1 | Ceramide synthase involved in sphingolipid metabolism |
| | RNA polymerase subunit beta | ATCG00190.1 | Constituent of RNA polymerase B |
| | Pre-mRNA-splicing factor SPF27 homologue | AT3G18165.1 | mRNA splicing of resistance genes |
| Ribosome/translation-related | Ribosomal protein L16 | ATCG00790.1 | Structural constituent of ribosome |
| | Ribosomal protein S26e family protein | AT2G40510.1 | Structural constituent of ribosome |
| | Ribosomal protein S8e family protein | AT5G59240.1 | Structural constituent of ribosome |
| | Ribosomal protein S2 | ATCG00160.1 | Structural constituent of ribosome |
| Protein ubiquitination | Eukaryotic translation initiation factor 3A | AT4G11420.1 | Constituent of eukaryotic initiation factor 3 |
| | F-box protein PP2-A13 | AT3G61060.1 | Protein ubiquitination |
| | BTB/POZ domain-containing protein | AT1G63850.1 | Protein ubiquitination |
| | Ubiquitin-conjugating enzyme 28 | AT1G64230.1 | Protein ubiquitination |
| Histone | Ubiquitin-like protein 5 | AT5G42300.1 | Ubiquitin-like modification |
| | Histone H2A.2 | AT3G20670.1 | Histones/DNA binding/nucleosome assembly |
| | Histone H3.3 | AT4G40030.2 | Histones/DNA binding/nucleosome assembly |
| Others | Photosystem II light harvesting complex gene 2.1 | AT2G05100.1 | Constituent of light harvesting complex II |
| | Alternative oxidase 1A | AT3G22370.1 | Alternative oxidase activity |
| | Tubulin folding cofactor D | AT3G60740.1 | Microtubule stability |
| | Asparagine synthetase 2 | AT5G65010.2 | Asparagine biosynthesis |
| | Glutamate-1-semialdehyde 2,1-aminomutase 2 | AT3G48730.1 | Porphyrin-containing compound metabolism |
| | Membrane-associated progesterone binding protein 3 | AT3G48890.1 | Porphyrin binding |
| | Thioredoxin superfamily protein | AT3G62950.1 | Electron carrier activity |
| | DNA polymerase epsilon catalytic subunit | AT1G08260.1 | DNA replication proofreading |
| | NAC domain containing protein 32 | AT1G77450.1 | Transcription factor |
| | DNA-binding protein phosphatase 1 | AT2G25620.1 | Protein phosphatase activity |
| | Protein kinase 1B | AT2G28930.1 | Serine/threonine kinase activity |
| | UDP-glycosyltransferase superfamily protein | AT5G04480.1 | — |
| | Adenine nucleotide alpha hydrolases-like superfamily protein | AT1G11360.4 | — |
| | Protein of unknown function (DUF300) | AT1G11200.1 | — |
| | Protein of unknown function (DUF803) | AT1G34470.1 | — |

Gene functions were predicted with corresponding Arabidopsis gene of highest sequence similarity.

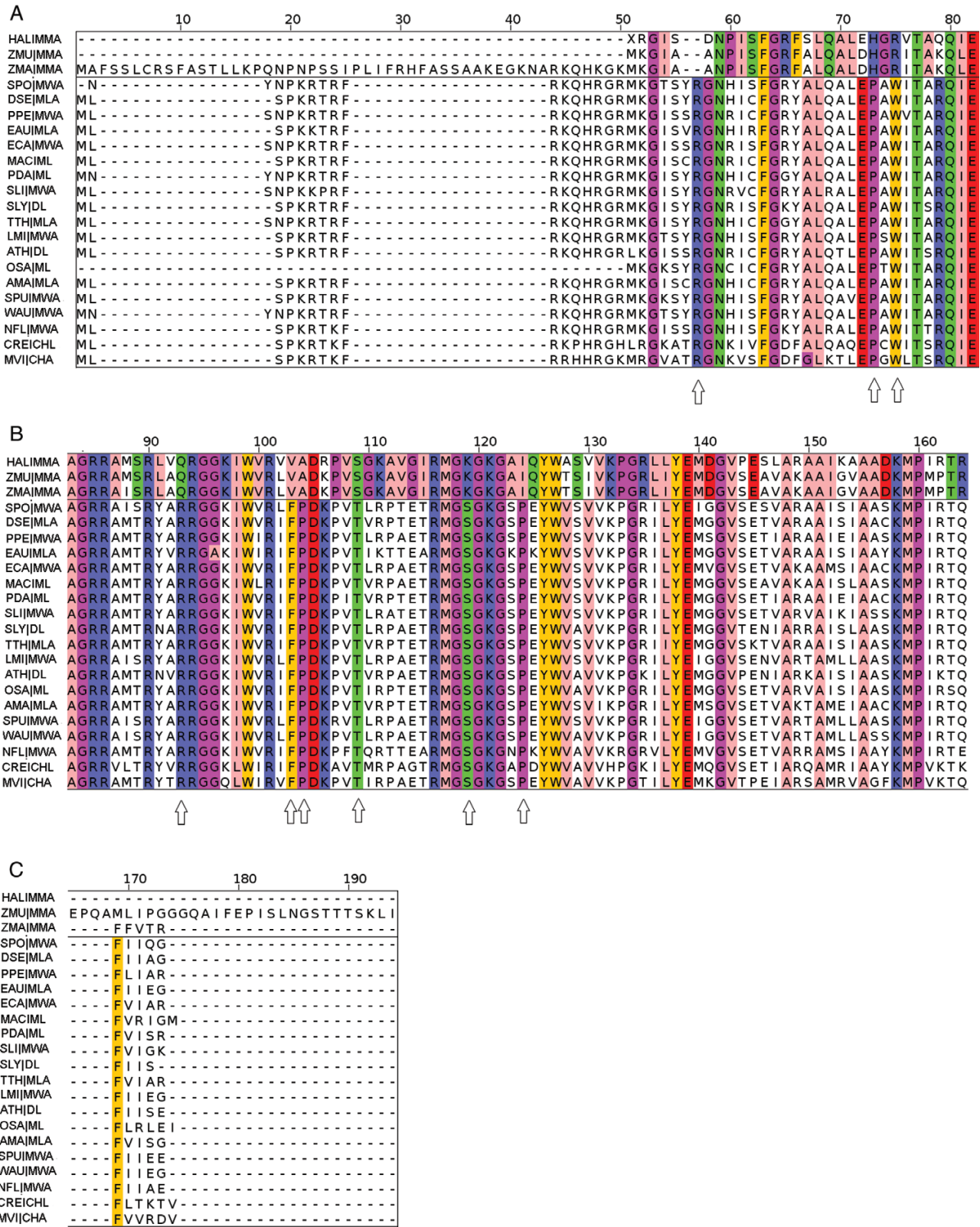


Fig. 2. Ribosomal protein L16 multiple sequence alignments between 19 species (AMA, *Alocasia macrorrhizos*; ATH, *Arabidopsis*; DSE, *Dieffenbachia seguine*; EAU, *Epiprenum aureum*; ECA, *Elodia canadensis*; LMI, *Lemna minor*; MAC, *Musa acuminata*; NFL, *Najas flexilis*; OSA, *Oryza sativa*; PDA, *Phoenix dactylifera*; PPE, *Potamogeton perfoliatus*; SLI, *Sagittaria lichuanensis*; SLY, *Solanum lycopersicum*; SPO, *Spirodela polyrrhiza*; SPU, *Spirodela pundata*; TTH, *Tofieldia thibetica*; WAU, *Wolffia australiana*) together with three seagrasses (HAL, *H. ovalis*; ZMA, *Z. marina*; ZMU, *Z. muelleri*). Species and corresponding IDs are listed in [Table S1](#). Amino acids that were conserved within the non-seagrass group or among seagrasses are coloured according to physicochemical properties based on 'Zappo' colour scheme. White arrows indicated seagrass-specific mutations.

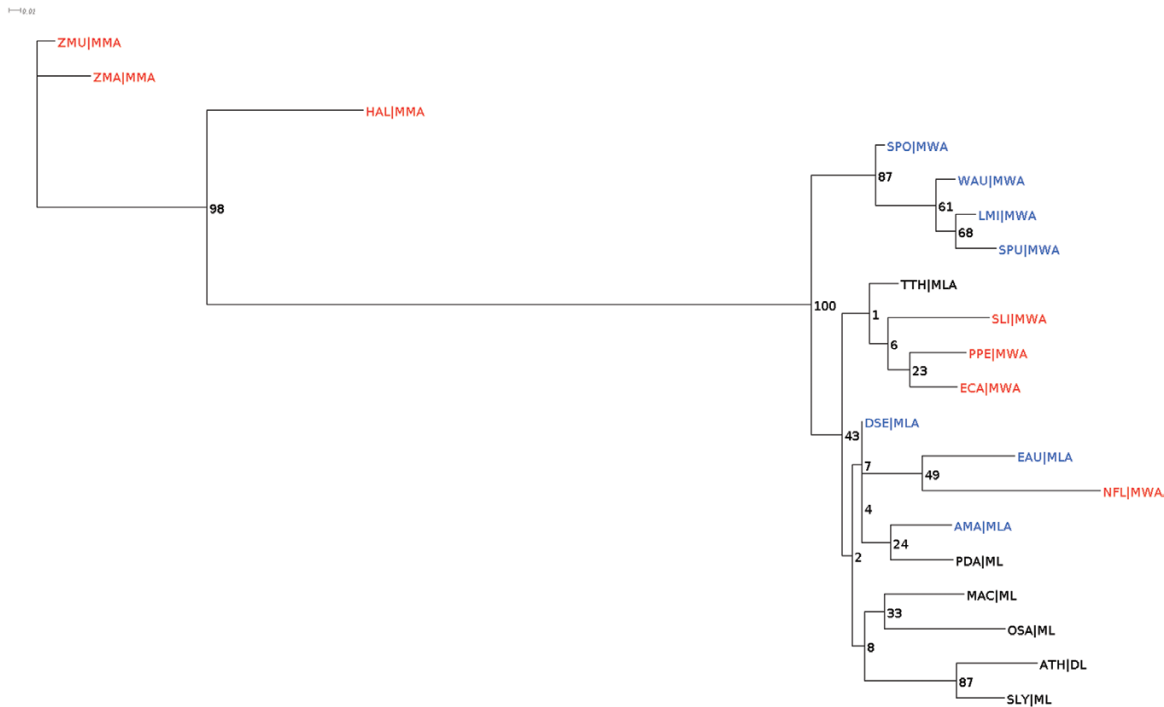


Fig. 3. Phylogenetic tree showing distance between ribosome protein L16 sequences of 17 species (AMA, *Alocasia macrorrhizos*; ATH, *Arabidopsis*; DSE, *Dieffenbachia seguine*; EAU, *Epiprenum aureum*; ECA, *Elodea canadensis*; LMI, *Lemna minor*; MAC, *Musa acuminata*; NFL, *Najas flexilis*; OSA, *Oryza sativa*; PDA, *Phoenix dactylifera*; PPE, *Potamogeton perfoliatus*; SLI, *Sagittaria lichuanensis*; SLY, *Solanum lycopersicum*; SPO, *Spirodela polyrrhiza*; SPU, *Spirodela pundata*; TTH, *Tofieldia thibetica*; WAU, *Wolffia australiana*) together with three seagrasses (HAL, *H. ovalis*; ZMA, *Z. marina*; ZMU, *Z. muelleri*). The order and habitat of species were indicated in the second part of each ID: DL, dicot, land; ML, monocot, land; MLA, monocot, land, Alismatales; MMA, monocot, marine, Alismatales; MWA, monocot, freshwater, Alismatales. Complete details are listed in Table S1. IDs coloured in red are members of core Alismatids, blue are members of Araceae, and black are others. Branches are labelled with bootstrap values (%).

shared by the three seagrass species despite belonging to two separate clades (Les *et al.*, 1997; Li and Zhou, 2009; Les and Tippery, 2013; Petersen *et al.*, 2016; Ross *et al.*, 2016). The possible convergence is highlighted by the absence of these mutations in representatives of sister genera for both clades. *Potamogeton perfoliatus* belongs to the tepaloid clade together with Zosteraceae, whereas *Najas flexilis*, *Elodea canadensis* and *Sagittaria lichuanensis* belong to the petaloid clade together with *H. ovalis* (Les *et al.*, 1997; Li and Zhou, 2009; Les and Tippery, 2013; Petersen *et al.*, 2016; Ross *et al.*, 2016). Protein sequences of L16 in these non-marine species have greater similarity with other monocots and dicots than with the seagrasses (Figs 2, 3) suggesting selection and convergent evolution to the marine habitat in seagrasses. Since *N. flexilis* and *P. perfoliatus* shared submergence characteristics with seagrasses, the mutations may be linked to salinity tolerance, rather than an ability to survive underwater. These results complement the seagrass clustering of OGCZ through OrthoMCL analysis and provided further molecular evidence of convergent evolution of seagrasses.

Differences between *H. ovalis* and the two Zosteraceae species were identified in genes encoding NDH, a major protein complex residing in the thylakoid membrane of chloroplasts that participates in cyclic electron flow pathways as an oxidoreductase (reviewed in Peltier *et al.*, 2016). As the NDH complex is only present in the Streptophyta lineage, which includes charophyte algae and land plants, acquisition of novel NDH genes likely occurred during terrestrial transition, and NDH is hypothesized to be one of the innovations enabling

land plant evolution (Martín *et al.*, 2009; Ruhlman *et al.*, 2015). The absence of genes encoding NDH subunits and proteins required for complex formation in *H. ovalis* points to a total loss of the NDH complex in the *H. ovalis* thylakoid. Rare evidence of loss or pseudogenization of plastid NDH genes has been reported in independent lineages (Wolfe *et al.*, 1992; Haberhausen and Zetsche, 1994; Funk *et al.*, 2007; Braukmann *et al.*, 2009; Logacheva *et al.*, 2011), including several genera in the Hydrocharitaceae family (Iles *et al.*, 2013; Peredo *et al.*, 2013; Wilkin and Mayo, 2013; Ross *et al.*, 2016). The observed loss of NDH genes in *H. ovalis* is the first report of their dispensability among Alismatales.

Several reasons for NDH dispensability have been suggested (Stefanović and Olmstead, 2005; Iles *et al.*, 2013; Peredo *et al.*, 2013; Xu *et al.*, 2013). Ross *et al.* (2016) suggest that NDH loss enabled low N investment as an adaptation to nutrient deficiency in the submerged environment. This is plausible, as *H. ovalis* is adapted to grow in low nutrient sediments (Carruthers *et al.*, 2007), and examples of nitrogen sources affecting NDH expression have been reported in green algae (Peltier and Schmidt, 1991). Interestingly, two proteins related to nitrate uptake, nitrogen reductase 1 (NR1) and nitrate transporter (NRT3.1) are also lost in *H. ovalis* (Table S4). One limitation of seagrass nitrogen uptake studies is that the potential contribution of microbial communities is not accounted for, and may be compensating for the loss of NDH in *H. ovalis*, as demonstrated in myco-heterotrophic liverworts (Wickett *et al.*, 2008a,b). Cyanobacteria on leaves have been shown to

contribute to nitrogen uptake in *Posidonia* (Jeremy Bougoure, personal communication). However, further targeted studies are required to determine whether the loss of the NDH complex in *H. ovalis* is related to nitrogen uptake.

Conclusion

Together, the conservation of gene loss and the sharing of seagrass-specific orthologues in these two independent lineages, despite the phylogenetic distance, has shed light on the genetics of marine adaptation in angiosperms of land plant ancestry. These results also present another example of habitat-driven parallel evolution in the plant kingdom.

Supplementary data

Supplementary data are available at *JXB* online.

Fig. S1. Venn diagram showing the number of shared orthologous clusters among six species (*Arabidopsis*, *M. acuminata*, *O. sativa*, *S. polyrhiza*, and two *Zosteraceae* species).

Table S1. Species selected for multiple sequence alignment of orthologous proteins.

Table S2. Number of *H. ovalis* reads sequenced and remaining after filtering process.

Table S3. List of TAIR genes that were conserved in OGCsM and at least one species among *H. ovalis*, *Z. muelleri*, and *Z. marina*.

Table S4. List of TAIR genes that were conserved in OGCsM but absent in at least one species among *H. ovalis*, *Z. muelleri*, and *Z. marina*.

Table S5. Significantly enriched biological process GO terms in the genes that were lost in *H. ovalis*, but present in *Z. muelleri*, *Z. marina*, and five other plant species.

Table S6. List of orthologous groups that are conserved in *Z. muelleri* and *Z. marina* (OGCZ).

Table S7. List of OGCZ orthologous groups that are conserved in *H. ovalis* and the best corresponding TAIR ID hit; each protein ID is followed by InterProScan IDs of domains found or no domain found (NA).

Acknowledgements

The authors would like to acknowledge funding support from the Australian Research Council (Projects LP160100030, LP140100537, LP130100925, LP110100200, and LP0989200). Support is also acknowledged from the Queensland Cyber Infrastructure Foundation (QCIF), the Pawsey Supercomputing Centre with funding from the Australian Government and the Government of Western Australia and resources from the National Computational Infrastructure (NCI), which is supported by the Australian Government.

References

Alexa A, Rahnenfuhrer J. 2010. topGO: Enrichment analysis for Gene Ontology. R package version 2.26.0. <http://bioconductor.uib.no/2.7/bioc/html/topGO.html>.

Aquino RS, Grativol C, Mourão PA. 2011. Rising from the sea: correlations between sulfated polysaccharides and salinity in plants. *PLoS One* **6**, e18862.

Aquino RS, Landeira-Fernandez AM, Valente AP, Andrade LR, Mourão PA. 2005. Occurrence of sulfated galactans in marine angiosperms: evolutionary implications. *Glycobiology* **15**, 11–20.

Asaoka R, Uemura T, Ito J, Fujimoto M, Ito E, Ueda T, Nakano A. 2013. *Arabidopsis* RABA1 GTPases are involved in transport between the trans-Golgi network and the plasma membrane, and are required for salinity stress tolerance. *The Plant Journal* **73**, 240–249.

Bankevich A, Nurk S, Antipov D, *et al.* 2012. SPAdes: a new genome assembly algorithm and its applications to single-cell sequencing. *Journal of Computational Biology* **19**, 455–477.

Brandizzi F, Barlowe C. 2013. Organization of the ER-Golgi interface for membrane traffic control. *Nature Reviews. Molecular Cell Biology* **14**, 382–392.

Braukmann TW, Kuzmina M, Stefanović S. 2009. Loss of all plastid *ndh* genes in Gnetales and conifers: extent and evolutionary significance for the seed plant phylogeny. *Current Genetics* **55**, 323–337.

Camacho C, Coulouris G, Avagyan V, Ma N, Papadopoulos J, Bealer K, Madden TL. 2009. BLAST+: architecture and applications. *BMC Bioinformatics* **10**, 421.

Cambridge ML, Zavala-Perez A, Cawthray GR, Mondon J, Kendrick GA. 2017. Effects of high salinity from desalination brine on growth, photosynthesis, water relations and osmolyte concentrations of seagrass *Posidonia australis*. *Marine Pollution Bulletin* **115**, 252–260.

Carpaneto A, Naso A, Paganetto A, Cornara L, Pesce ER, Gambale F. 2004. Properties of ion channels in the protoplasts of the Mediterranean seagrass *Posidonia oceanica*. *Plant Cell and Environment* **27**, 279–292.

Carruthers TJB, Dennison WC, Kendrick GA, Waycott M, Walker DI, Cambridge ML. 2007. Seagrasses of south-west Australia: a conceptual synthesis of the world's most diverse and extensive seagrass meadows. *Journal of Experimental Marine Biology and Ecology* **350**, 21–45.

Chen LY, Chen JM, Gituru RW, Wang QF. 2012. Generic phylogeny, historical biogeography and character evolution of the cosmopolitan aquatic plant family Hydrocharitaceae. *BMC Evolutionary Biology* **12**, 30.

Chen LY, Shi DQ, Zhang WJ, Tang ZS, Liu J, Yang WC. 2015. The *Arabidopsis* alkaline ceramidase TOD1 is a key turgor pressure regulator in plant cells. *Nature Communications* **6**, 6030.

Chikhi R, Medvedev P. 2014. Informed and automated *k*-mer size selection for genome assembly. *Bioinformatics* **30**, 31–37.

Coyer JA, Hoarau G, Kuo J, Tronholm A, Veldsink J, Olsen JL. 2013. Phylogeny and temporal divergence of the seagrass family *Zosteraceae* using one nuclear and three chloroplast loci. *Systematics and Biodiversity* **11**, 271–284.

Driouich A, Faye L, Staehelin LA. 1993. The plant Golgi apparatus: a factory for complex polysaccharides and glycoproteins. *Trends in Biochemical Sciences* **18**, 210–214.

Driouich A, Follet-Gueye ML, Bernard S, Kousar S, Chevalier L, Vitré-Gibouin M, Lerouxel O. 2012. Golgi-mediated synthesis and secretion of matrix polysaccharides of the primary cell wall of higher plants. *Frontiers in Plant Science* **3**, 79.

Fellows I. 2014. wordcloud: Word Clouds. R package version 2.5. <https://CRAN.R-project.org/package=wordcloud>.

Fukushima K, Fang X, Alvarez-Ponce D, *et al.* 2017. Genome of the pitcher plant *Cephalotus* reveals genetic changes associated with carnivory. *Nature Ecology & Evolution* **1**, 59.

Funk HT, Berg S, Krupinska K, Maier UG, Krause K. 2007. Complete DNA sequences of the plastid genomes of two parasitic flowering plant species, *Cuscuta reflexa* and *Cuscuta gronovii*. *BMC Plant Biology* **7**, 45.

Gasteiger E, Gattiker A, Hoogland C, Ivanyi I, Appel RD, Bairoch A. 2003. ExPASy: The proteomics server for in-depth protein knowledge and analysis. *Nucleic Acids Research* **31**, 3784–3788.

Golicz AA, Schliep M, Lee HT, Larkum AW, Dolferus R, Batley J, Chan CK, Sablok G, Ralph PJ, Edwards D. 2015. Genome-wide survey of the seagrass *Zostera muelleri* suggests modification of the ethylene signalling network. *Journal of Experimental Botany* **66**, 1489–1498.

Guindon S, Delsuc F, Dufayard JF, Gascuel O. 2009. Estimating maximum likelihood phylogenies with PhyML. *Methods in Molecular Biology* **537**, 113–137.

Haberhausen G, Zetsche K. 1994. Functional loss of all *ndh* genes in an otherwise relatively unaltered plastid genome of the holoparasitic flowering plant *Cuscuta reflexa*. *Plant Molecular Biology* **24**, 217–222.

- Hannun YA, Obeid LM. 2008. Principles of bioactive lipid signalling: lessons from sphingolipids. *Nature Reviews. Molecular Cell Biology* **9**, 139–150.
- Hasegawa PM. 2013. Sodium (Na⁺) homeostasis and salt tolerance of plants. *Environmental and Experimental Botany* **92**, 19–31.
- Hidalgo O, Garcia S, Garnatje T, Mumburá M, Patterson A, Vigo J, Vallès J. 2015. Genome size in aquatic and wetland plants: fitting with the large genome constraint hypothesis with a few relevant exceptions. *Plant Systematics and Evolution* **301**, 1927–1936.
- Huang R, O'Donnell AJ, Barboline JJ, Barkman TJ. 2016. Convergent evolution of caffeine in plants by co-option of exapted ancestral enzymes. *Proceedings of the National Academy of Sciences, USA* **113**, 10613–10618.
- Iles WJD, Smith SY, Graham SW. 2013. A well-supported phylogenetic framework for the monocot order Alismatales reveals multiple losses of the plastid NADH dehydrogenase complex and a strong long-branch effect. *Early Events in Monocot Evolution* **83**, 1–28.
- Jones P, Binns D, Chang HY, et al. 2014. InterProScan 5: genome-scale protein function classification. *Bioinformatics* **30**, 1236–1240.
- Joshi N, Fass J. 2011. Sickle: A sliding-window, adaptive, quality-based trimming tool for FastQ files (Version 1.33). <https://github.com/najoshi/sickle>.
- Katoh K, Misawa K, Kuma K, Miyata T. 2002. MAFFT: a novel method for rapid multiple sequence alignment based on fast Fourier transform. *Nucleic Acids Research* **30**, 3059–3066.
- Kawashima T, Lorković ZJ, Nishihama R, Ishizaki K, Axelsson E, Yelagandula R, Kohchi T, Berger F. 2015. Diversification of histone H2A variants during plant evolution. *Trends in Plant Science* **20**, 419–425.
- Khotimchenko Y, Khozhaenko E, Kovalev V, Khotimchenko M. 2012. Cerium binding activity of pectins isolated from the seagrasses *Zostera marina* and *Phyllospadix iwatensis*. *Marine Drugs* **10**, 834–848.
- Kirsch M, An Z, Viereck R, Löw R, Rausch T. 1996. Salt stress induces an increased expression of V-type H⁺-ATPase in mature sugar beet leaves. *Plant Molecular Biology* **32**, 543–547.
- Koch MS, Schopmeyer SA, Kyhn-Hansen C, Madden CJ, Peters JS. 2007. Tropical seagrass species tolerance to hypersalinity stress. *Aquatic Botany* **86**, 14–24.
- Kuo J, den Hartog C. 2006. Seagrass morphology, anatomy, and ultrastructure. In: Larkum AWD, Orth RJ, Duarte CM, eds. *Seagrasses: Biology, Ecology and Conservation*. Dordrecht: Springer, 51–87.
- Larkum AWD, Orth RJ, Duarte CM. 2006. *Seagrasses: biology, ecology and conservation*. Dordrecht: Springer.
- Lee H, Golicz AA, Bayer PE, et al. 2016. The genome of a southern hemisphere seagrass species (*Zostera muelleri*). *Plant Physiology* **172**, 272–283.
- Lerouxel O, Cavalier DM, Liepman AH, Keegstra K. 2006. Biosynthesis of plant cell wall polysaccharides—a complex process. *Current Opinion in Plant Biology* **9**, 621–630.
- Les DH, Cleland MA, Waycott M. 1997. Phylogenetic studies in Alismatidae, II: evolution of marine angiosperms (seagrasses) and hydrophyly. *Systematic Botany* **22**, 443–463.
- Les DH, Tippery NP. 2013. In time and with water ... the systematics of alismatid monocotyledons. *Early Events in Monocot Evolution* **83**, 118–164.
- Li L, Stoeckert CJ Jr, Roos DS. 2003. OrthoMCL: identification of ortholog groups for eukaryotic genomes. *Genome Research* **13**, 2178–2189.
- Li XX, Zhou ZK. 2009. Phylogenetic studies of the core Alismatales inferred from morphology and *rbcL* sequences. *Progress in Natural Science* **19**, 931–945.
- Logacheva MD, Schelkunov MI, Penin AA. 2011. Sequencing and analysis of plastid genome in mycoheterotrophic orchid *Neottia nidus-avis*. *Genome Biology and Evolution* **3**, 1296–1303.
- Martín M, Funk HT, Serrot PH, Poltnigg P, Sabater B. 2009. Functional characterization of the thylakoid Ndh complex phosphorylation by site-directed mutations in the *ndhF* gene. *Biochimica et Biophysica Acta* **1787**, 920–928.
- Miserey-Lenkei S, Chalancon G, Bardin S, Formstecher E, Goud B, Echard A. 2010. Rab and actomyosin-dependent fission of transport vesicles at the Golgi complex. *Nature Cell Biology* **12**, 645–654.
- Nguyen XV, Hofler S, Glasenapp Y, Thangaradjou T, Lucas C, Papenbrock J. 2015. New insights into DNA barcoding of seagrasses. *Systematics and Biodiversity* **13**, 496–508.
- Olsen JL, Rouzé P, Verhelst B, et al. 2016. The genome of the seagrass *Zostera marina* reveals angiosperm adaptation to the sea. *Nature* **530**, 331–335.
- Ord TJ, Summers TC. 2015. Repeated evolution and the impact of evolutionary history on adaptation. *BMC Evolutionary Biology* **15**, 137.
- Ovodov YS, Ovodova RG, Bondaren OD, Krasikov IN. 1971. The pectic substances of *zosteraceae*: Part IV. Pectinase digestion of zosterine. *Carbohydrate Research* **18**, 311–318.
- Paterson AH, Lin YR, Li Z, Schertz KF, Doebley JF, Pinson SR, Liu SC, Stansel JW, Irvine JE. 1995. Convergent domestication of cereal crops by independent mutations at corresponding genetic loci. *Science* **269**, 1714–1718.
- Peltier G, Aro EM, Shikanai T. 2016. NDH-1 and NDH-2 plastoquinone reductases in oxygenic photosynthesis. *Annual Review of Plant Biology* **67**, 55–80.
- Peltier G, Schmidt GW. 1991. Chlororespiration: an adaptation to nitrogen deficiency in *Chlamydomonas reinhardtii*. *Proceedings of the National Academy of Sciences, USA* **88**, 4791–4795.
- Peredo EL, King UM, Les DH. 2013. The plastid genome of *Najas flexilis*: adaptation to submersed environments is accompanied by the complete loss of the NDH complex in an aquatic angiosperm. *PLoS One* **8**, e68591.
- Petersen G, Seberg O, Cuenca A, Stevenson DW, Thadeo M, Davis JI, Graham S, Ross TG. 2016. Phylogeny of the Alismatales (Monocotyledons) and the relationship of *Acorus* (Acorales?). *Cladistics* **32**, 141–159.
- Rausell A, Kanhonou R, Yenush L, Serrano R, Ros R. 2003. The translation initiation factor eIF1A is an important determinant in the tolerance to NaCl stress in yeast and plants. *The Plant Journal* **34**, 257–267.
- Ross TG, Barrett CF, Soto Gomez M, et al. 2016. Plastid phylogenomics and molecular evolution of Alismatales. *Cladistics* **32**, 160–178.
- Ruhlman TA, Chang WJ, Chen JJ, et al. 2015. NDH expression marks major transitions in plant evolution and reveals coordinate intracellular gene loss. *BMC Plant Biology* **15**, 100.
- Short FT, Polidoro B, Livingstone SR, et al. 2011. Extinction risk assessment of the world's seagrass species. *Biological Conservation* **144**, 1961–1971.
- Slater GS, Birney E. 2005. Automated generation of heuristics for biological sequence comparison. *BMC Bioinformatics* **6**, 31.
- Stefanović S, Olmstead RG. 2005. Down the slippery slope: plastid genome evolution in Convolvulaceae. *Journal of Molecular Evolution* **61**, 292–305.
- Strydom S, McMahon K, Kendrick GA, Statton J, Lavery PS. 2017. Seagrass *Halophila ovalis* is affected by light quality across different life history stages. *Marine Ecology Progress Series* **572**, 103–116.
- Taji T, Seki M, Satou M, Sakurai T, Kobayashi M, Ishiyama K, Narusaka Y, Narusaka M, Zhu JK, Shinozaki K. 2004. Comparative genomics in salt tolerance between *Arabidopsis* and *Arabidopsis*-related halophyte salt cress using *Arabidopsis* microarray. *Plant Physiology* **135**, 1697–1709.
- Tao JJ, Chen HW, Ma B, Zhang WK, Chen SY, Zhang JS. 2015. The role of ethylene in plants under salinity stress. *Frontiers in Plant Science* **6**, 1059.
- Touchette BW. 2007. Seagrass-salinity interactions: physiological mechanisms used by submersed marine angiosperms for a life at sea. *Journal of Experimental Marine Biology and Ecology* **350**, 194–215.
- Touchette BW, Marcus SE, Adams EC. 2014. Bulk elastic moduli and solute potentials in leaves of freshwater, coastal and marine hydrophytes. Are marine plants more rigid? *AoB Plants* **6**, plu014.
- Valente C, Polishchuk R, De Matteis MA. 2010. Rab6 and myosin II at the cutting edge of membrane fission. *Nature Cell Biology* **12**, 635–638.
- van Meer G, Voelker DR, Feigenson GW. 2008. Membrane lipids: where they are and how they behave. *Nature Reviews. Molecular Cell Biology* **9**, 112–124.
- Voesenek LACJ, Pierik R, Sasidharan R. 2015. Plant life without ethylene. *Trends in Plant Science* **20**, 783–786.
- Washburn JD, Bird KA, Conant GC, Pires JC. 2016. Convergent evolution and the origin of complex phenotypes in the age of systems biology. *International Journal of Plant Sciences* **177**, 305–318.
- Waterhouse AM, Procter JB, Martin DM, Clamp M, Barton GJ. 2009. Jalview version 2—a multiple sequence alignment editor and analysis workbench. *Bioinformatics* **25**, 1189–1191.

- Weraduwage SM, Kim SJ, Renna L, C Anozie F, D Sharkey T, Brandizzi F.** 2016. Pectin methylesterification impacts the relationship between photosynthesis and plant growth. *Plant Physiology* **171**, 833–848.
- Wickett NJ, Fan Y, Lewis PO, Goffinet B.** 2008a. Distribution and evolution of pseudogenes, gene losses, and a gene rearrangement in the plastid genome of the nonphotosynthetic liverwort, *Aneura mirabilis* (Metzgeriales, Jungermanniopsida). *Journal of Molecular Evolution* **67**, 111–122.
- Wickett NJ, Zhang Y, Hansen SK, Roper JM, Kuehl JV, Plock SA, Wolf PG, DePamphilis CW, Boore JL, Goffinet B.** 2008b. Functional gene losses occur with minimal size reduction in the plastid genome of the parasitic liverwort *Aneura mirabilis*. *Molecular Biology and Evolution* **25**, 393–401.
- Wilkin P, Mayo SJ.** 2013. *Early Events in Monocot Evolution*. Cambridge: Cambridge University Press.
- Wissler L, Codoñer FM, Gu J, Reusch TB, Olsen JL, Procaccini G, Bornberg-Bauer E.** 2011. Back to the sea twice: identifying candidate plant genes for molecular evolution to marine life. *BMC Evolutionary Biology* **11**, 8.
- Wolfe KH, Morden CW, Palmer JD.** 1992. Function and evolution of a minimal plastid genome from a nonphotosynthetic parasitic plant. *Proceedings of the National Academy of Sciences, USA* **89**, 10648–10652.
- Xu L, Law SR, Murcha MW, Whelan J, Carrie C.** 2013. The dual targeting ability of type II NAD(P)H dehydrogenases arose early in land plant evolution. *BMC Plant Biology* **13**, 100.
- Ye CJ, Zhao KF.** 2003. Osmotically active compounds and their localization in the marine halophyte eelgrass. *Biologia Plantarum* **46**, 137–140.
- Zhang M, Smith JA, Harberd NP, Jiang C.** 2016. The regulatory roles of ethylene and reactive oxygen species (ROS) in plant salt stress responses. *Plant Molecular Biology* **91**, 651–659.
- Zhu C, Ganguly A, Baskin TI, McClosky DD, Anderson CT, Foster C, Meunier KA, Okamoto R, Berg H, Dixit R.** 2015. The fragile Fiber1 kinesin contributes to cortical microtubule-mediated trafficking of cell wall components. *Plant Physiology* **167**, 780–792.